KYBERNETIKA — VOLUME *55* (2019), NUMBER 2, PAGES 402–421

A SWINGING UP CONTROLLER FOR THE FURUTA PENDULUM BASED ON THE TOTAL ENERGY CONTROL SYSTEM APPROACH

H. Rodríguez-Cortés

This paper considers the problem of swinging up the Furuta pendulum and proposes a new smooth nonlinear swing up controller based on the concept of energy. This new controller results from the Total Energy Control System (TECS) approach in conjunction with a linearizing feedback controller. The new controller commands to the desired reference the total energy rate of the Furuta pendulum; thus, the Furuta pendulum oscillates and reaches a neighborhood of its unstable configuration while the rotation of its base remains bounded. Once the Furuta pendulum configuration is in the neighborhood of its unstable equilibrium point, a linear controller stabilizes the unstable configuration of the Furuta pendulum. Real-time experiments are included to support the theoretical developments.

Keywords: total energy control system, Furuta pendulum, swinging up control, real-time experiments

Classification: 93C10, 93C15

1. INTRODUCTION

The mechanical structure of the Furuta pendulum is composed of two arms. The first arm, actuated by an electric motor, rotates parallel to the horizontal plane. The second arm, the pendulum, hangs at the tip of the first arm and rotates without actuation around the axis of the first arm. The Furuta pendulum dynamics represent an uncomplicated version of complex dynamics arising in challenging applications such as flexible robotic systems, aerial vehicles, and aerospace systems; thus the Furuta pendulum is a popular benchmark to test different control techniques.

From the control theory point of view, the Furuta pendulum is a mechanical system with characteristics that appeal researchers, among them, under actuation, open-loop instability of the upright equilibrium position and states with non-linear configuration spaces. The angular positions of the Furuta pendulum have configuration spaces that are not homeomorphic to the Euclidean space; thus no continuous vector field on these configuration spaces have a global asymptotic equilibrium point [15]. Failing to interpret the stability properties of a controller designed using local coordinates in the global configuration space could lead to the unwinding phenomenon [6]. Due to its complex

DOI: 10.14736/kyb-2019-2-0402

topology, the approach to obtain a global solution for the Furuta pendulum is through hybrid controllers. The controller that locally stabilizes the straight equilibrium point is joined, using a switching strategy, to a second controller. The second controller swings up the pendulum from the downward balance point to a neighborhood of the upright equilibrium point.

The linear approximation of the Furuta pendulum dynamics at its unstable configuration is controllable [8]. As a result, the control problem of stabilizing this unstable equilibrium can be locally solved employing linear control techniques. Nonlinear controllers are proposed to enhance the region of attraction of linear control designs. The Furuta pendulum dynamics can be transformed to a nontriangular quadratic normal form [23]. Thus, the unstable equilibrium point of the Furuta pendulum can be semiglobally asymptotically stabilized using a Fixed Point Controller [22]. Following the controlled Lagrangians method in [7], a feedback stabilization controller for the Furuta pendulum is synthesized with a computable region of attraction. Recently, several control algorithms to stabilize the unstable equilibrium point without considering the swinging up procedure have been proposed. For example, the works in [5] using the integral sliding mode technique, in [1] applying input-output linearization, and in [24] employing proportional-retarded control. The literature, sometimes, employs the term inverted pendulum to refer to the Furuta pendulum as well as to the inverted pendulum on a cart. However, as shown in [23] both dynamical systems have different structural properties. Almost global controllers, for the inverted pendulum on a cart, are presented, for example in [2] using energy shaping methods and smooth switching between positive and negative feedback, and in [21] using a change of coordinates and using backstepping. The work in [18] introduces an output feedback controller to stabilize the unstable configuration of the pendulum on a cart based on an extended high gain observer and multi-time-scale controller structure. Reference [25] solves the stabilization problem for the inverted pendulum on a cart using Linear quadratic regulator (LQR) and proportional-integral-derivative (PID) methods.

The concept of energy is at the core of most of the swing up controllers. Reference [4] presents a quite detailed description of an energy-based controller to swing up the Furuta pendulum. This energy-based controller does not take into account the dynamics of the actuated degree of freedom; thus, this coordinate may have an unbounded behavior. In [10], the authors propose an interpretation of the energy-based controller of [4] concerning the Fradkov's Speed-Gradient. Additionally, the authors propose a swing up approach that considers the complete model of the Furuta pendulum. Thus, it is possible to prescribe a bounded behavior to the actuated coordinate. The work in [3] generalizes the construction of dynamic invariants for the Furuta pendulum; then using the Speed-Gradient method a new swing up strategy is designed. New homoclinic curves are constructed using virtual holonomic constraints in [12] and [27]; then conditions guaranteeing the existence of solutions surrounding such curves are given. A swing up control scheme that injects energy, based on the exponentiation of the pendulum's angular position, is proposed in [26]. The injected energy is minimal when the pendulum's angular position is close to the upright equilibrium point. The brief in [13] suggests an optimal swing up and stabilization controller for the Furuta pendulum based on the stable manifold method. In this brief, the stable manifold method approximately

solves the Hamilton-Jacobi equation that results from the swing up and stabilization optimal control problem. The work in [11] proposes a swing up algorithm for a double pendulum on a cart based on the inversion-based feedforward control. The swing up problem for the triple inverted pendulum on a cart is addressed in [9]. The proposed swing up algorithm is based on a nonlinear feedforward controller and an optimal feedback controller.

A. A. Lambregts introduced the TECS method as a control technique to command the longitudinal dynamics of a fixed-wing aircraft in [16, 17]. The foundation of the TECS approach is the construction of two signals called the total energy rate and the energy distribution rate. It turns out that these two signals are proportional to the time derivatives of two functions strongly related to the concept of energy. The TECS method proposes to command these two outputs to their desired reference using a proportional-integral (PI) controller. An interesting point of this control technique is that it adequately models the way that pilots manage kinetic and potential energy when they fly a plane. A. A. Lambregts proposed TECS at the end of the eighties, however, to the best knowledge of the author; this control technique remained in the field of control of aerial vehicles. Hence, the developments in this paper are the first effort to apply TECS in other scenarios.

This paper considers the problem of swinging up the Furuta pendulum and proposes a new smooth nonlinear swing up controller based on the concept of energy. The new controller results from the Total Energy Control System (TECS) approach in conjunction with a linearizing feedback controller. Regarding the TECS method, the proposed controller commands, to the desired reference, the total energy rate of the Furuta pendulum. Thus, the Furuta pendulum oscillates and reaches a neighborhood of its unstable configuration while the rotation of its base remains bounded. Once the Furuta pendulum arrangement is in the neighborhood of its unstable equilibrium point, a linear controller stabilizes the unstable configuration of the Furuta pendulum. Real-time experiments are included to support the theoretical developments.

The proposed algorithm belongs to the class of swing up controllers based on the concept of energy. While in [10] and [3] the desired energy function and the desired energy-like are specified, respectively, here the desired total energy rate is defined. On the works in [27] and [12] where the desired homoclinic curves are constructed through the virtual holonomic constraints, here the homoclinic curve arises from defining the desired total energy rate.

The developments in this document have the following structure. Section 2 introduces the Furuta pendulum dynamic model as well as a feedback linearization controller to simplify the dynamics. Section 3 gives a brief description of the Total Energy Control System approach in a general setting. Section 4 presents the developments carried out to obtain the controller that swings up the Furuta pendulum. Section 5 shows a set of experiments to evaluate the performance of the proposed swing up technique. Section 6 completes the paper with some concluding remarks.

2. DYNAMIC MODEL OF THE FURUTA PENDULUM

Figure 1 shows the Furuta pendulum. Inside the cubical base, there is an electric motor that actuates the angular position of the first arm θ. The cylinder contains an encoder

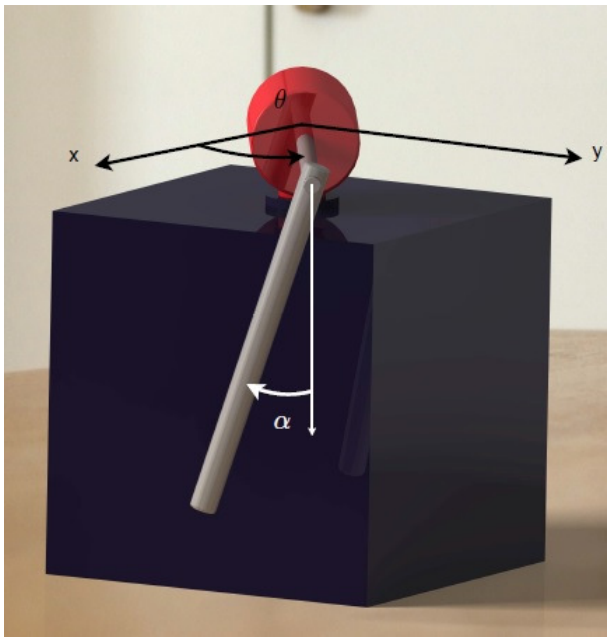

Fig. 1. Furuta pendulum.

to measure the angular position of the pendulum α. The angular position α is the non-actuated coordinate. The dynamic model of the Furuta pendulum is available in the literature. Following any of the available modeling methods such as Newton second law, the Lagrangian or Hamiltonian formalisms or the bond graph method, it is straightforward to obtain a dynamic model of the Furuta pendulum. The following set of non-linear equations describes the dynamics of the Furuta pendulum

$$\begin{aligned} \left(J_p + \frac{1}{4}M_pL_p^2\right)\ddot{\alpha} + \frac{1}{2}M_pL_pL_r\cos(\alpha)\ddot{\theta} & \\ -\frac{1}{4}M_pL_p^2\cos(\alpha)\sin(\alpha)\dot{\theta}^2 + \frac{1}{2}M_pL_pg\sin(\alpha) &= 0 \\ \left(M_pL_r^2 + \frac{1}{4}M_pL_p^2\sin(\alpha)^2 + J_r\right)\ddot{\theta} + \frac{1}{2}M_pL_pL_r\cos(\alpha)\ddot{\alpha} & \\ +\frac{1}{2}M_pL_p^2\sin(\alpha)\cos(\alpha)\dot{\theta}\dot{\alpha} - \frac{1}{2}M_pL_pL_r\sin(\alpha)\dot{\alpha}^2 + \frac{k_tk_m}{R_m}\dot{\theta} &= \frac{k_t}{R_m}V_m \end{aligned} \tag{1}$$

where J_p, M_p and L_p are the inertia, the mass, and the length of the pendulum, respectively. J_r and L_r are the inertia and the length of the first arm, respectively. Moreover, k_t is the torque constant of the electric motor, k_m is the motor back-EMF and R_m is the rotor terminal resistance. Additionally, g is the acceleration of gravity and V_m is the control input, the applied voltage to the electric motor.

The following set is the configuration space of the coordinates that describe the

dynamics of the Furuta pendulum

$$\mathcal{D} = \{\mathcal{S} \times \mathcal{S} \times \mathbb{R} \times \mathbb{R}\}$$

with $\mathcal{S}$ the unit circle. The use of local coordinates may introduce singularities and ambiguities that can be avoided using a geometric formulation for systems evolving in configuration spaces non homeomorphic to the Euclidean space as presented in [19].

To simplify the dynamics of the Furuta pendulum, assuming that all states are measurable and all parameters are known, the following linearizing control feedback is defined

$$\begin{aligned} V_m &= \frac{M_p^2 L_p^2 L_r R_m}{2k_t(4J_p + M_p L_p^2)} \cos(\alpha)\sin(\alpha)\left(L_p \cos(\alpha)\dot{\theta}^2 - 2g\right) \\ &\quad + \frac{M_p L_p^2 R_m}{2k_t}\cos(\alpha)\sin(\alpha)\dot{\alpha}\dot{\theta} + \frac{R_m}{k_t}\left[M_p L_r^2 + \frac{1}{4}M_p L_p^2(1-\cos(\alpha)^2) + J_r \right. \\ &\quad \left. - \frac{M_p^2 L_p^2 L_r^2}{4J_p + M_p L_p^2}\cos(\alpha)^2\right]\left(\frac{L_p}{2L_r}\sin(\alpha)\dot{\theta}^2 + \bar{V}_m\right) - \frac{M_p L_p L_r R_m}{2k_t}\sin(\alpha)\alpha^2 + k_m\dot{\theta} \end{aligned} \tag{2}$$

with $\bar{V}_m$ a new control input. The Furuta pendulum dynamics (1) in closed-loop with the control input (2) takes the following form

$$\begin{aligned} \bar{J}\ddot{\alpha} + M_p L_p g \sin(\alpha) &= -M_p L_p L r \cos(\alpha)\bar{V}_m \\ \ddot{\theta} - \frac{L_p}{2L_r}\sin(\alpha)\dot{\theta}^2 &= \bar{V}_m \end{aligned} \tag{3}$$

where

$$\bar{J} = 2J_p + \frac{1}{2}M_p L_p^2$$

Note that it is possible to rewrite equation (3) as follows

$$\begin{aligned} \bar{J}\ddot{\alpha} + M_p L_p g \sin(\alpha) &= -M_p L_p L r \cos(\alpha)\ddot{\theta} \\ &\quad + M_p L_p L r \cos(\alpha)\frac{L_p}{2L_r}\sin(\alpha)\dot{\theta}^2 \end{aligned} \tag{4}$$

The developments in [4] consider the next simplified version of the dynamic model given in equation (4)

$$(2J_p + \frac{1}{2}M_p L_p^2)\ddot{\alpha} + M_p L_p g \sin(\alpha) = -M_p L_p L r \cos(\alpha)\ddot{\theta} \tag{5}$$

where the control input is $\ddot{\theta}$. The disadvantage of considering $\ddot{\theta}$ as the control input is that the displacement of the base of the Furuta pendulum could go beyond its physical limits [10]. This document considers the dynamic model (3) to design the swing up controller.

3. THE TECS METHOD

The next paragraphs present a brief description of the TECS method in a general framework.

Consider a mechanical system described by port Hamiltonian equations [28]

$$\begin{bmatrix} \dot{q} \\ \dot{p} \end{bmatrix} = \begin{bmatrix} 0 & I \\ -I & 0 \end{bmatrix} \begin{bmatrix} \nabla_q \mathcal{H} \\ \nabla_p \mathcal{H} \end{bmatrix} + \begin{bmatrix} 0 \\ G(q) \end{bmatrix} u \tag{6}$$

with $q \in \mathcal{M} \subset \mathbb{R}^n$ the generalized coordinate, $p \in \mathbb{R}^n$ the generalized momentum, $u \in \mathbb{R}^n$ the control input, I the $n \times n$ identity matrix and $G(q) \in \mathbb{R}^{n \times n}$ the input matrix, assumed to be full rank. Additionally, $\mathcal{H}(q,p)$ is the Hamiltonian function given by

$$\mathcal{H}(q,p) = \frac{1}{2} p^\top M(q)^{-1} p + V(q) \tag{7}$$

with $M(q)$ the inertia matrix and $V(q)$ the potential energy function. The Lagrangian function associated to (6) and (7) is

$$\mathcal{L}(q,\dot{q}) = \frac{1}{2} \dot{q}^\top M(q) \dot{q} - V(q) \tag{8}$$

Using the Legendre transform $p = M(q)\dot{q}$, with a slight abuse of notation, the Lagrangian function expressed in generalized position and momentum coordinates takes the form

$$\mathcal{L}(q,p) = \frac{1}{2} p^\top M(q)^{-1} p - V(q) \tag{9}$$

Note that the time derivatives of the Hamiltonian function (7), and the Lagrangian function (8) along the port-Hamiltonian system (6) can be written as follows

$$\begin{aligned} \dot{\mathcal{H}} &= p^\top M(q)^{-1} \left[\dot{p} + \frac{1}{2} \nabla_q \left(p^\top M(q)^{-1} p \right) + \nabla_q V(q) \right] \\ \dot{\mathcal{L}} &= p^\top M(q)^{-1} \left[\dot{p} + \frac{1}{2} \nabla_q \left(p^\top M(q)^{-1} p \right) - \nabla_q V(q) \right] \end{aligned} \tag{10}$$

According to references, [16] and [17], the total energy rate and the energy distribution rate are defined as

$$\begin{aligned} \mathcal{H}_e &= \dot{p} + \frac{1}{2} \nabla_q \left(p^\top M(q)^{-1} p \right) + \nabla_q V(q) \\ \mathcal{L}_e &= \dot{p} + \frac{1}{2} \nabla_q \left(p^\top M(q)^{-1} p \right) - \nabla_q V(q) \end{aligned}$$

Straightforward computations show that the following relationships hold

$$\begin{aligned} \mathcal{H}_e &= G(q)u \\ \mathcal{L}_e &= G(q)u - 2\nabla_q V(q) \end{aligned}$$

The TECS approach proposes to command the total energy and distribution energy rates to desired references. The control objective determines the desired references for $\mathcal{H}_e$ and $\mathcal{L}_e$.

Assume that, for this developments, the control objective is to command q and p to desired references q_d and 0, respectively. Thus, the total energy and distribution energy rate errors acquire the following shape

$$\begin{aligned} \tilde{\mathcal{H}}_e &= \dot{p} + K_p p + \nabla_q V(\tilde{q}) \\ \tilde{\mathcal{L}}_e &= \dot{p} + K_p p - \nabla_q V(\tilde{q}) \end{aligned} \tag{11}$$

where

$$\begin{aligned} \tilde{\mathcal{H}}_e &= \mathcal{H}_e - \mathcal{H}_e^d \\ \tilde{\mathcal{L}}_e &= \mathcal{L}_e - \mathcal{L}_e^d \\ \tilde{q} &= q - q_d \end{aligned}$$

with

$$\begin{aligned} \mathcal{H}_e^d &= -K_p p + \frac{1}{2}\nabla_q \left(p^\top M(q)^{-1} p\right) + \nabla_q V(q) - \nabla_q V(\tilde{q}) \\ \mathcal{L}_e^d &= -K_p p + \frac{1}{2}\nabla_q \left(p^\top M(q)^{-1} p\right) - \nabla_q V(q) + \nabla_q V(\tilde{q}) \end{aligned}$$

and K_p a control gain. The references $\mathcal{H}_e^d$ and $\mathcal{L}_e^d$ are designed to shape the form of the equations in (11). Note that convergence of both equations in (11) to zero ensures the accomplishment of the control objective. Hence, if it is possible to design a control law such that

$$\lim_{t\to\infty} \tilde{\mathcal{H}}_e = 0, \ \lim_{t\to\infty} \tilde{\mathcal{L}}_e = 0 \tag{12}$$

then

$$\lim_{t\to\infty} \nabla_q V(\tilde{q}) = 0$$

and

$$\lim_{t\to\infty} (\dot{p} + K_p p) = 0$$

thus, if $V(\tilde{q})$ has a minimum at $\tilde{q} = 0$ the controller will achieve the objective at least locally.

TECS approach proposes to achieve (12) using a proportional-integral controller in terms of the error signals (11). However, to synthesize the PI controller, it is necessary to consider the zero relative degree of the error signals (11). Additionally, it could happen that there are not enough control inputs to command both error signals. In [16, 17], it is possible to control both error signals to zero, because the longitudinal aircraft dynamics has two inputs and the total energy and the distribution energy rates are scalar functions. In an application of TECS method to control the translational dynamics of a quadrotor, only one of the TECS error signals is commanded to zero [29]. When it is not possible to command both total energy and distribution energy error rates to zero, it is mandatory to modify the definition of the error rates to ensure that the control objective can be accomplished. Here, it is proposed to command the total energy rate. Thus, the total energy rate error is modified as follows

$$\tilde{\mathcal{H}}_e = \dot{p} + K_p p + \nabla_q V(\tilde{q}) + K_q \tilde{q}$$

with K_q a control gain. Thus, the TECS controller reads as

$$u = K_P \tilde{\mathcal{H}}_e + K_I \int_0^t \tilde{\mathcal{H}}_e(\tau)\,\mathrm{d}\tau \tag{13}$$

with K_P and K_I the PI control gains.

Since $\tilde{\mathcal{H}}_e$ has zero relative degree, the controller u in (8) is not explicitly defined. Assuming that the matrix $I - K_P G(q)$ has full rank, an explicit definition of the controller is given by

$$\begin{aligned} u &= [I - K_P G(q)]^{-1} \left\{ K_P \left[\nabla_q V(\tilde{q}) + K_p p + K_q \tilde{q} - \frac{1}{2} \nabla_q \left(p^\top M(q)^{-1} p \right) - \nabla_q V(q) \right] \right. \\ &\quad \left. + K_I \mathcal{H}_e^i \right\} \end{aligned} \tag{14}$$

with

$$\mathcal{H}_e^i = \int_0^t \tilde{\mathcal{H}}_e(\tau)\,\mathrm{d}\tau$$

At the level of generality of this example, it is hard to state stability properties of the port-Hamiltonian system (6) in closed-loop with the TECS controller (14). Note that the closed-loop dynamics described by the following equations does not preserve any particular structure.

$$\begin{aligned} \dot{\tilde{q}} &= M(\tilde{q} + q_d)^{-1} p \\ \dot{p} &= -\left\{ I + G(\tilde{q} + q_d) \left[I - K_P G(\tilde{q} + q_d) \right]^{-1} K_P \right\} \left[\frac{1}{2} \nabla_q \left(p^\top M(\tilde{q} + q_d)^{-1} p \right) \right. \\ &\quad \left. + \nabla_q V(\tilde{q} + q_d) \right] + G(\tilde{q} + q_d) \left[I - K_P G(\tilde{q} + q_d) \right]^{-1} K_P \left[\nabla_q V(\tilde{q}) + K_p p + K_p \tilde{q} \right] \\ &\quad + G(\tilde{q} + q_d) \left[I - K_P G(\tilde{q} + q_d) \right]^{-1} K_I \mathcal{H}_e^i \\ \dot{\mathcal{H}}_e^i &= -\left\{ I + G(\tilde{q} + q_d) \left[I - K_P G(\tilde{q} + q_d) \right]^{-1} K_P \right\} \left[\frac{1}{2} \nabla_q \left(p^\top M(\tilde{q} + q_d)^{-1} p \right) \right. \\ &\quad \left. + \nabla_q V(\tilde{q} + q_d) \right] + G(\tilde{q} + q_d) \left[I - K_P G(\tilde{q} + q_d) \right]^{-1} K_P \left[\nabla_q V(\tilde{q}) + K_p p + K_p \tilde{q} \right] \\ &\quad + G(\tilde{q} + q_d) \left[I - K_P G(\tilde{q} + q_d) \right]^{-1} K_I \mathcal{H}_e^i + K_p p + \nabla_q V(\tilde{q}) + K_q \tilde{q} \end{aligned} \tag{15}$$

Hence, to verify that the TECS controller achieves the control objective. It is necessary to check that the closed-loop dynamics (15) has an equilibrium point at the desired position. The equilibrium points for the dynamic system (15) are the solutions of the following set of algebraic equations.

$$\begin{aligned} 0 &= M(\tilde{q} + q_d)^{-1} p \\ 0 &= -\left\{ I + G(\tilde{q} + q_d) \left[I - K_P G(\tilde{q} + q_d) \right]^{-1} K_P \right\} \left[\frac{1}{2} \nabla_q \left(p^\top M(\tilde{q} + q_d)^{-1} p \right) \right. \\ &\quad \left. + \nabla_q V(\tilde{q} + q_d) \right] + G(\tilde{q} + q_d) \left[I - K_P G(\tilde{q} + q_d) \right]^{-1} K_P \left[\nabla_q V(\tilde{q}) + K_p p + K_p \tilde{q} \right] \\ &\quad + G(\tilde{q} + q_d) \left[I - K_P G(\tilde{q} + q_d) \right]^{-1} K_I \mathcal{H}_e^i \\ 0 &= K_p p + \nabla_q V(\tilde{q}) + K_q \tilde{q} \end{aligned} \tag{16}$$

From the first and the last equations in (16), assuming that $V(\tilde{q})$ has a minimum at $\tilde{q}$, it follows that $p = 0$ and $\tilde{q} = 0$. Then, the set of algebraic equations in (16) reduces to the following equation

$$0 = -\left\{I + G(q_d)\left[I - K_P G(q_d)\right]^{-1} K_P\right\} \nabla_q V(q_d) + G(q_d)\left[I - K_P G(q_d)\right]^{-1} K_I \mathcal{H}_e^i$$

This equation defines the steady-state value of $\mathcal{H}_e^i$. Finally, appealing to linear control techniques, it is necessary to verify that the closed-loop dynamics (15) is asymptotically stable at the desired equilibrium point.

Once the total energy rate reference is defined, the time derivative of the Hamiltonian function (10) takes the following form

$$\dot{\mathcal{H}} = p^\top M(q)^{-1}\left[\tilde{\mathcal{H}}_e + \mathcal{H}_e^d\right]$$

thus, the classical interpretation of the time derivative of the Hamiltonian function in terms of the passivity concept does not directly follows. Note that

$$\lim_{\tilde{\mathcal{H}}_e \to 0} \dot{\mathcal{H}} = p^\top M(q)^{-1} \mathcal{H}_e^d$$

at the desired equilibrium point $q = q_d$ and $p = 0$ one has

$$\lim_{\tilde{\mathcal{H}}_e \to 0} \dot{\mathcal{H}} = 0$$

The interpretation of TECS method in terms of other energy based control techniques passivity, for example, is an open issue. Even though these technical problems the TECS method solves the trajectory tracking problem for a quadrotor in [29] and, in this paper the TECS method will produce a controller to swing up the Furuta pendulum.

4. SWING UP CONTROLLER

This section presents the design procedure of a controller based on the TECS approach to swing up the pendulum to a neighborhood of its vertical position. Consider the closed-loop dynamics of the Furuta pendulum described by equation (3). The total energy function for the non-actuated coordinate is given by

$$\mathcal{H} = \frac{1}{2}\bar{J}\dot{\alpha}^2 + M_p L_p g\left[1 - \cos(\alpha)\right] \tag{17}$$

It is easy to verify that the time derivative of the total energy function (17) can be written as follows

$$\dot{\mathcal{H}} = \bar{J} g \dot{\alpha}\left[\frac{\ddot{\alpha}}{g} + \frac{M_p L_p}{\bar{J}}\sin(\alpha)\right]$$

Following the TECS strategy, the total energy rate reads as

$$\mathcal{H}_e = \frac{\ddot{\alpha}}{g} + \frac{M_p L_p}{\bar{J}}\sin(\alpha)$$

Along the trajectories of the dynamic system (3) the total energy rate can be expressed as follows

$$\mathcal{H}_e = -\frac{M_p L_p}{\bar{J}} \frac{L_r}{g} \cos(\alpha) \bar{V}_m \tag{18}$$

According to the TECS method, the next step is to define a desired reference for the total energy rate. The control objective must be to generate harmonic motion for the no actuated coordinate, to swing up the Furuta pendulum. It can be noticed that with $\bar{V}_m = 0$, it follows that

$$\ddot{\alpha} + \frac{g}{L_e} \sin(\alpha) = 0 \tag{19}$$

with $L_e = \dfrac{\bar{J}}{M_p L_p}$, thus; the dynamic system (19) describes a periodic motion for small oscilations $\sin(\alpha) \approx \alpha$. However, selecting $\bar{V}_m$ equal zero does not allow to modify the periodic motion described by (19). To influence the periodic motion, through the control input $\bar{V}_m$, the desired total energy rate is defined as

$$\mathcal{H}_e^d = -\frac{\kappa}{L_e} \Phi(\alpha) \sin(\alpha)$$

with

$$\Phi(\alpha) = \frac{\cos(\alpha)^2}{1 + \cos(\alpha)^2} \tag{20}$$

and κ a positive constant. The function (20) is introduced to deal with the fact that the control input $\bar{V}_m$ enters to the first equation of (3) multiplying a cosine function. The energy rate error reads as

$$\tilde{\mathcal{H}}_e = \frac{\ddot{\alpha}}{g} + \frac{1}{L_e} \left[1 + \kappa \Phi(\alpha)\right] \sin(\alpha) \tag{21}$$

with $\tilde{\mathcal{H}}_e = \mathcal{H}_e - \mathcal{H}_e^d$. Combining equation (18) with equation (21) one obtains

$$\tilde{\mathcal{H}}_e = -\frac{1}{L_e} \frac{L_r}{g} \cos(\alpha) \bar{V}_m + \frac{\kappa}{L_e} \Phi(\alpha) \sin(\alpha)$$

Defining

$$\bar{V}_m = \kappa \frac{g}{L_r} \frac{\cos(\alpha)}{1 + \cos(\alpha)^2} \sin(\alpha) \tag{22}$$

it follows that

$$\tilde{\mathcal{H}}_e = \frac{\ddot{\alpha}}{g} + \frac{1}{L_e} \left[1 + \kappa \Phi(\alpha)\right] \sin(\alpha) = 0 \tag{23}$$

The controller (22) in closed-loop with (4) generates the following differential equations

$$\begin{aligned} \ddot{\alpha} + \frac{g}{L_e} \left[1 + \kappa \Phi(\alpha)\right] \sin(\alpha) &= 0 \\ \ddot{\theta} - \frac{L_p}{2 L_r} \sin(\alpha) \dot{\theta}^2 &= \kappa \frac{g}{L_r} \frac{\cos(\alpha)}{1 + \cos(\alpha)^2} \sin(\alpha) \end{aligned} \tag{24}$$

The first equation in (24) can be interpreted as a Hamiltonian system of the form (6) with Hamiltonian function defined by

$$\mathcal{H}_a = \frac{1}{2}\dot{\alpha}^2 + V_a(\alpha)$$

and

$$V_a(\alpha) = \frac{g}{L_e}\left\{1 + \frac{4-\pi}{2}\kappa - (1+2\kappa)\cos(\alpha) + 2\kappa \arctan\left[\cos(\alpha)\right]\right\}$$

It is easy to verify that

$$\mathcal{H}_a = \frac{1}{2}\dot{\alpha}^2 + V_\alpha(\alpha)$$

is an invariant for (14). Thus, $\mathcal{H}_a$ defines a homoclinic orbit for the dynamics in (14). Additionally, the gain κ can modify the shape of the homoclinic orbit. Now, to limit the motion of the pendulum's base, the controller (13) is modified as follows

$$\bar{V}_m = \kappa \frac{g}{L_r}\frac{\cos(\alpha)}{1+\cos(\alpha)^2}\sin(\alpha) - k_\theta \dot{\theta}$$

with k_θ a control gain.

Hence, the closed-loop dynamics reads as

$$\begin{aligned} \ddot{\alpha} + \beta\left[1 + \kappa\Phi(\alpha)\right]\sin(\alpha) &= \frac{L_r\beta}{g}\cos(\alpha)k_\theta\dot{\theta} \\ \ddot{\theta} - \frac{L_p}{2L_r}\sin(\alpha)\dot{\theta}^2 &= \kappa\frac{g}{L_r}\frac{\cos(\alpha)}{1+\cos(\alpha)^2}\sin(\alpha) - k_\theta\dot{\theta} \end{aligned} \tag{25}$$

with $\beta = \frac{g}{L_e}$. All previous developments do not take into account damping forces. Using experiments, in the next Section, the effect of the damping forces will be included. In addition, it will be shown that the proposed controller achieves the control objective.

5. EXPERIMENTAL RESULTS

The experimental results were performed with the QUBE Servo prototype from Quanser [14]. The Qube Servo prototype consists of two Allied Motion, model 16705, brushed DC motors. The rotating arm is driven by a pulse width modulation (PWM) signal. The Data Acquisition (DAQ) device, connected to a personal computer (PC) via USB, generates such a PWM signal. The US Digital rotary optical shaft, model E8P-512-118, generates 2048 counts per revolution to measure the angular positions of the rotating arm and the pendulum. Both encoders are connected to the DAQ. The proposed swing up controller is implemented using the Quanser Real-Time Control (QUARC) software. The parameters of the Furuta pendulum are: $M_p = 0.24$kg, $L_p = 0.129$m, $L_r = 0.085$m, $J_p = 3.3282 \times 10^{-5}$kgm^2, $J_r = 5.7198 \times 10^{-5}$kgm^2, $R_m = 8.4\,\Omega$, $k_t = 0.042$ Nm/A, $k_m = 0.042$ Vs/rad, $g = 9.81$ m/s^2.

The first experiment shows that considering $\kappa = 0$, the control objective is not satisfied as the oscilations vanish. The solution of the linear approximation of (25), at

$\alpha = \dot{\alpha} = 0$ and $\theta = \dot{\theta} = 0$ for initial conditions $\alpha(0)$, $\dot{\alpha}(0)$, $\theta(0)$ and $\dot{\theta}(0)$ and $\kappa = 0$ is given by

$$\begin{aligned}
\alpha(t) &= \frac{\sqrt{\beta}k_\theta^2 L_r\dot{\theta}(0) + g\sqrt{\beta}(\dot{\alpha}(0) + k_\theta^2\dot{\alpha}(0))}{g(k_\theta^2+\beta)}\sin(\sqrt{\beta}t) + \frac{\beta L_r k_\theta\dot{\theta}(0)}{g(k_\theta^2+\beta)}e^{-k_\theta t} \\
&\quad + \frac{\beta(g\alpha(0) - L_r k_\theta\dot{\theta}(0)) + gk_\theta^2\alpha(0)}{g(k_\theta^2+\beta)}\cos(\sqrt{\beta}t) \\
\dot{\alpha}(t) &= \frac{\beta(k_\theta^2 L_r\dot{\theta}(0) + g\dot{\alpha}(0)) + gk_\theta^2\dot{\alpha}(0)}{g(k_\theta^2+\beta)}\cos(\sqrt{\beta}t) - \frac{k_\theta^2\beta L_r\dot{\theta}(0)}{g(k_\theta^2+\beta)}e^{-k_\theta t} \\
&\quad - \frac{\beta^{\frac{3}{2}}(g\alpha(0) - L_r k_\theta\dot{\theta}(0)) + g\sqrt{\beta}k_\theta^2\alpha(0)}{g(k_\theta^2+\beta)}\sin(\sqrt{\beta}t) \\
\theta(t) &= -\frac{1}{k_\theta}\dot{\theta}(0)(1 - e^{-k_\theta t}) + \theta(0) \\
\dot{\theta}(t) &= \dot{\theta}(0)e^{-k_\theta t}
\end{aligned}$$

thus, it seems that the pendulum will swing up until it reaches a neighborhood of the vertical equilibrium if one selects the right initial conditions. Note that selecting $\alpha(0)$, $\dot{\alpha}(0)$, $\theta(0)$ and $\dot{\theta}(0)$ different from zero the solution converges to

$$\begin{aligned}
\alpha(t) &= \frac{\sqrt{\beta}k_\theta^2 L_r\dot{\theta}(0) + g\sqrt{\beta}(\dot{\alpha}(0) + k_\theta^2\dot{\alpha}(0))}{g(k_\theta^2+\beta)}\sin(\sqrt{\beta}t) \\
&\quad + \frac{\beta(g\alpha(0) - L_r k_\theta\dot{\theta}(0)) + gk_\theta^2\alpha(0)}{g(k_\theta^2+\beta)}\cos(\sqrt{\beta}t) \\
\dot{\alpha}(t) &= \frac{\beta(k_\theta^2 L_r\dot{\theta}(0) + g\dot{\alpha}(0)) + gk_\theta^2\dot{\alpha}(0)}{g(k_\theta^2+\beta)}\cos(\sqrt{\beta}t) \\
&\quad - \frac{\beta^{\frac{3}{2}}(g\alpha(0) - L_r k_\theta\dot{\theta}(0)) + g\sqrt{\beta}k_\theta^2\alpha(0)}{g(k_\theta^2+\beta)}\sin(\sqrt{\beta}t) \\
\theta(t) &= \theta(0) \\
\dot{\theta}(t) &= 0
\end{aligned}$$

Figure 2 shows the time history of the angular position of the pendulum as well as the control input. Note that the motion of α vanishes. Figure 3 presents the phase plane of the pendulum states, with $\kappa = 1.15$ and $k_\theta = 0$, as well as the angular position of the pendulum's base. Notice that the pendulum oscillates, however the angular position of the pendulum's base has a transient motion that may take it off the limits of the prototype. Additionally, the swing up of the pendulum is not close enough to the vertical position.

In order to show the effect of the control gain k_θ on the motion of the pendulum's base, this gain is now different from zero. Figure 4 shows the results for $\kappa = 1.15$ and $k_\theta = 49.5$. The gain k_θ helps in two ways, it reduces the transient motion of the pendulum's base and it increases the magnitude of the oscillation. Figure 5 shows the control input.

In the last experiment, the control algorithm adds a linear controller to stabilize the upright position of the pendulum. Thus, when the pendulum's position satisfies the condition $\alpha + \pi < |0.2|$rad, the balancing linear controller commands the prototype. Figure 6 shows the phase plane, note that after swinging up the pendulums converges to

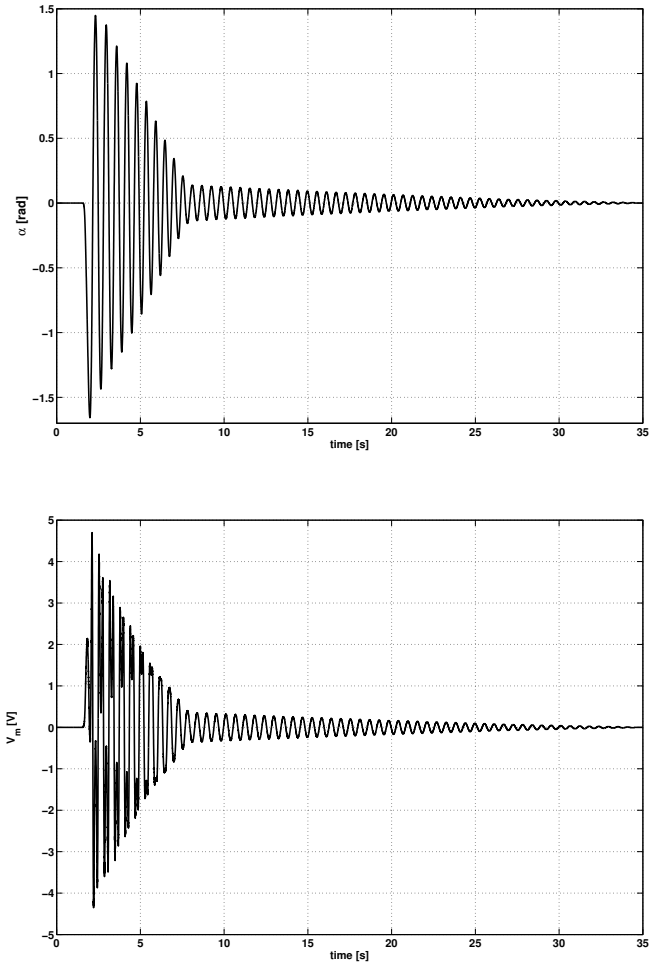

Fig. 2. Experimental results with $\kappa = 0$ and $k_\theta = 49.5$. Angular position α (top), control input V_m (bottom).

the vertical position. In this phase plane, the zero position for the pendulum corresponds to the downward configuration. Thus, the vertical position is on π radians. Figure 7 shows that the position of the pendulum's base remains bounded and it does not have big transients. Additionally, Figure 7 reports the time history of the control input. Finally, Figure 8 presents the total energy rate error which satisfies equation (23)

By comparing the proposed swing up strategy with energy based reported procedures, it is possible to state the following remarks. The controller developed in [4] becomes equal to zero at $\alpha = \pi/2$ and $\dot{\alpha} = 0$; the strategy proposed in this paper only equals

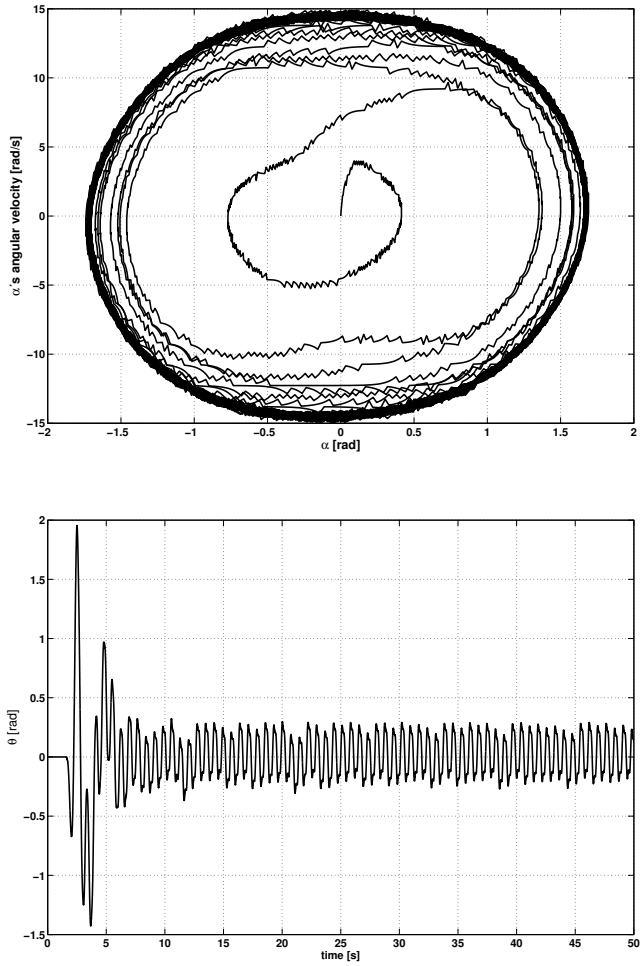

Fig. 3. Experimental results with $\kappa = 1.15$ and $k_\theta = 0$. Phase plane α vs $\dot{\alpha}$ (top), angular position θ (bottom).

to zero at $\alpha = \pi/2$. Looking at equation 2.4 of [3], one determines that the swing up controller becomes equal to zero at a complex combination of the Furuta pendulum states. The control philosophy followed in [4, 10], and [20] was to command the energy function, or an energy-like function, in [3], to the desired reference. The philosophy of the controller of this paper is to modify the internal dynamics described by equation (15). A performance index for swinging up controllers may be the number of swings to achieve the region of attraction of the local controller. For such a performance index the controller proposed in [4] is the best one because in a countable number of swings

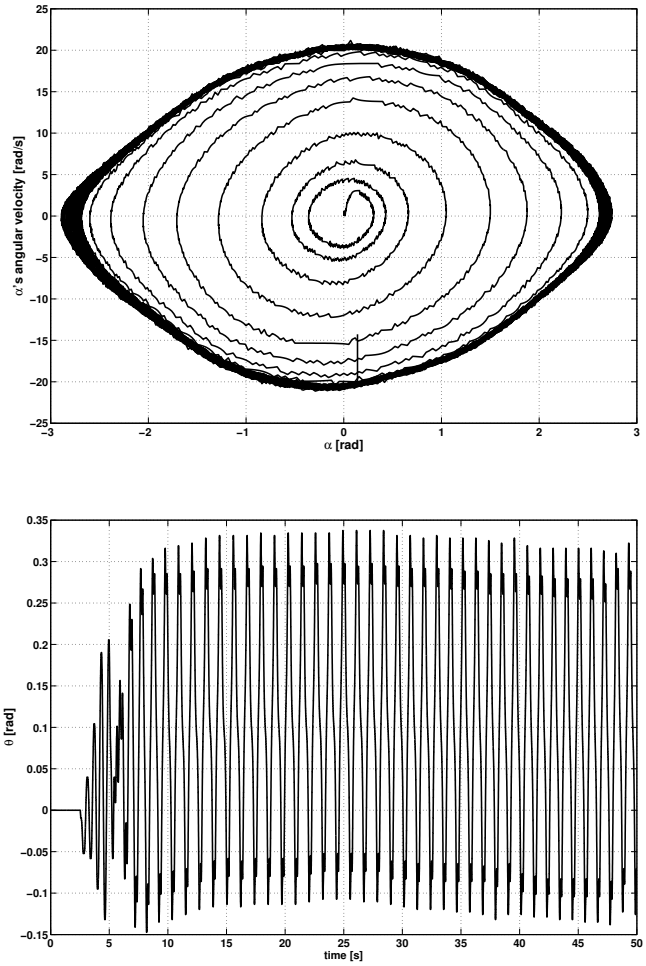

Fig. 4. Experimental results with $\kappa = 1.15$ and $k_\theta = 49.5$. Phase plane α vs $\dot{\alpha}$ (top), angular position θ (bottom).

achieves such a region. Moreover, concerning the complexity of the control strategy, the controller reported in [4] is also the simplest.

The links `http://youtu.be/ELWHPiMkvUI` and `http://youtu.be/FrhrxuI6sSM` show videos of the experiments corresponding to Figures 4 and 6, respectively.

6. CONCLUSION

This paper presents a generalization of the Total Energy Control System methodology for fully actuated mechanical systems. Then the proposed generalization is employed in

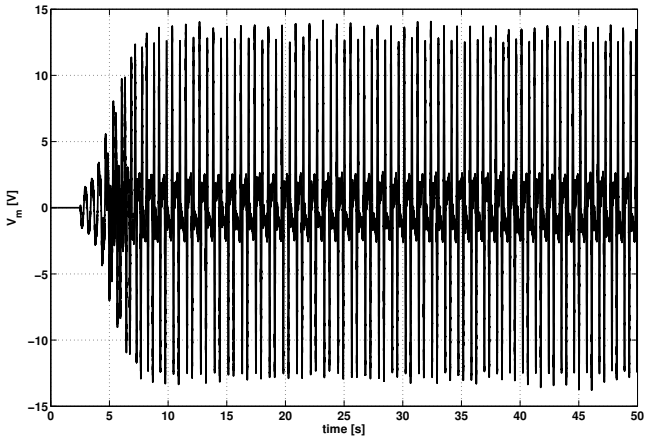

Fig. 5. Experimental results with $\kappa = 1.15$ and $k_\theta = 49.5$. Control input V_m.

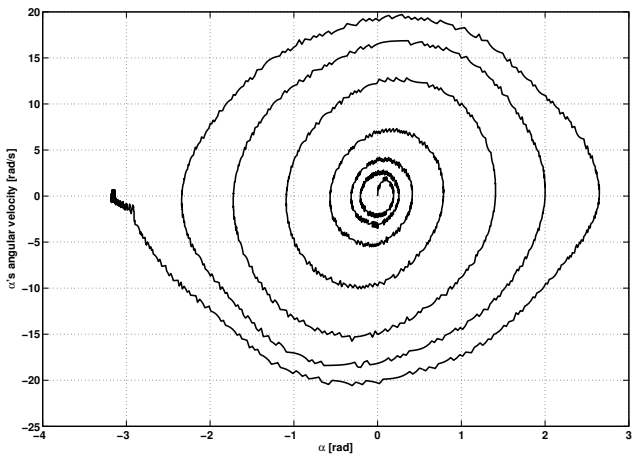

Fig. 6. Experimental results with $\kappa = 1.15$ and $k_\theta = 49.5$. Phase plane α vs $\dot{\alpha}$.

conjunction with a feedback linearization controller to design a strategy to swinging up the Furuta pendulum. A local controller stabilizes the Furuta pendulum at its upright configuration. Experimental results show that the proposed swing up algorithm works appropriately.

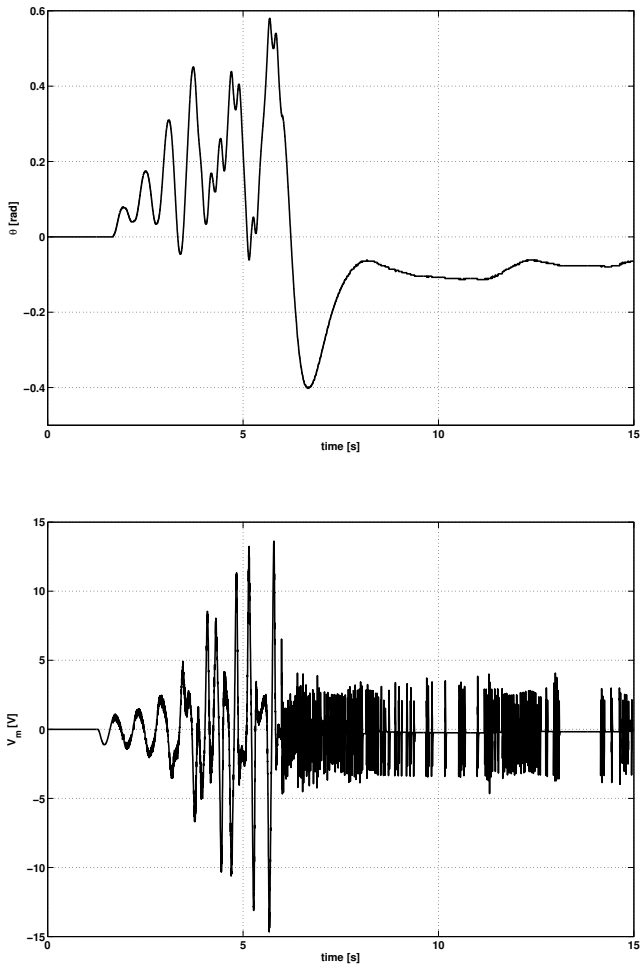

Fig. 7. Experimental results with $\kappa = 1.5$ and $k_\theta = 49.5$. Pendulum's base angular position θ (top), control input V_m (bottom).

CONFLICT OF INTEREST DISCLOSURE

The author declares that there is no conflict of interest regarding the publication of this paper.

(Received December 8, 2017)

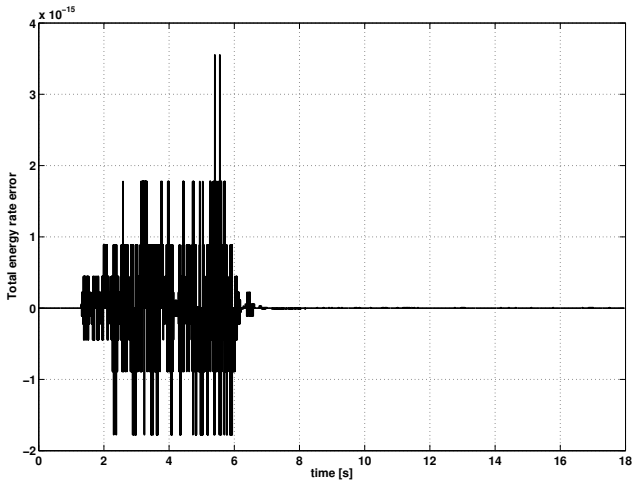

Fig. 8. Experimental results with $\kappa = 1.5$ and $k_\theta = 49.5$. Total energy rate error $\tilde{\mathcal{H}}_e$.

REFERENCES

[1] C. Aguilar-Avelar and J. Moreno-Valenzuela: New feedback linearization-based control for arm trajectory tracking of the furuta pendulum. IEEE/ASME Trans. Mechatron. *21* (2016), 2, 638–648. DOI:10.1109/tmech.2015.2485942

[2] D. Angeli: Almost global stabilization of the inverted pendulum via continuous state feedback. Automatica *37* (2001), 7, 1103–1108. DOI:10.1016/s0005-1098(01)00064-4

[3] J. Aracil, J. A. Acosta, and F. Gordillo: A nonlinear hybrid controller for swinging-up and stabilizing the furuta pendulum. Control Engrg. Practice *21* (2013), 8, 989–993. DOI:10.1016/j.conengprac.2013.04.001

[4] K. J. Åström and K. Furuta: Swinging up a pendulum by energy control. Automatica *36* (2002), 2, 287–295. DOI:10.1016/s0005-1098(99)00140-5

[5] A. T. Azar and F. E. Serrano: Adaptive Sliding Mode Control of the Furuta Pendulum. Springer International Publishing, Cham 2015, pp. 1–42. DOI:10.1007/978-3-319-11173-5_1

[6] S. P. Bhat and D. S. Bernstein: A topological obstruction to continuous global stabilization of rotational motion and the unwinding phenomenon. Systems Control Lett. *39* (2000), 1, 63–70. DOI:10.1016/s0167-6911(99)00090-0

[7] A. M. Bloch, N. E. Leonard, and J. E. Marsden: Stabilization of the pendulum on a rotor arm by the method of controlled lagrangians. In: Proc. IEEE International Conference on Robotics and Automation 1999, Vol. 1, IEEE 1999, pp. 500–505. DOI:10.1109/robot.1999.770026

[8] R. C. Dorf and R. H. Bishop: Modern Control Systems. Pearson, 2011.

[9] T. Gluck, A. Eder, and A. Kugi: Swing-up control of a triple pendulum on a cart with experimental validation. Automatica *49* (2013), 3, 801–808. DOI:10.1016/j.automatica.2012.12.006

[10] F. Gordillo, J. A. Acosta, and J. Aracil: A new swing-up law for the furuta pendulum. Int. J. Control *76* (2003), 8, 836–844. DOI:10.1080/0020717031000116506

[11] K. Graichen, M. Treuer, and M. Zeitz: Swing-up of the double pendulum on a cart by feedforward and feedback control with experimental validation. Automatica *43* (2007), 1, 63–71. DOI:10.1016/j.automatica.2006.07.023

[12] P. X. La Hera, L. B. Freidovich, A. S. Shiriaev, and U. Mettin: New approach for swinging up the furuta pendulum: Theory and experiments. Mechatronics *19* (2009), 8, 1240–1250. DOI:10.1016/j.mechatronics.2009.07.005

[13] T. Horibe and N. Sakamoto: Optimal swing up and stabilization control for inverted pendulum via stable manifold method. IEEE Trans. Control Systems Technol. *26* (2918), 2, 708–715. DOI:10.1109/tcst.2017.2670524

[14] Quanser Consulting Inc.: Qube servo, 2015. accessed: 2015-06-30.

[15] D. E. Koditschek: The application of total energy as a lyapunov function for mechanical control systems. Contemporary Math. *97* (1989), 131. DOI:10.1090/conm/097/1021035

[16] A. A. Lambregts: Integrated system design for flight and propulsion control using total energy principles. In: American Institute of Aeronautics and Astronautics, Aircraft Design, Systems and Technology Meeting, Fort Worth *17* (1983). DOI:10.2514/6.1983-2561

[17] A. A. Lambregts: Vertical flight path and speed control autopilot design using total energy principles. AIAA *83-2239* (1983). DOI:10.2514/6.1983-2561

[18] J. Lee, R. Mukherjee, and H. K. Khalil: Output feedback stabilization of inverted pendulum on a cart in the presence of uncertainties. Automatica *54* (2015), 146–157. DOI:10.1016/j.automatica.2015.01.013

[19] T. Lee, M. Leok, and H. McClamroch: Geometric formulations of furuta pendulum control problems. Math. Engrg., Science and Aerospace (MESA) *7* (2016), 1.

[20] R. Lozano, I. Fantoni, and D. J. Block: Stabilization of the inverted pendulum around its homoclinic orbit. Systems Control Lett. *40* (2000), 3, 197–204. DOI:10.1016/s0167-6911(00)00025-6

[21] F. Mazenc and L. Praly: Adding integrations, saturated controls, and stabilization for feedforward systems. IEEE Trans. Automat. Control *41* (1996), 11, 1559–1578. DOI:10.1109/9.543995

[22] R. Olfati-Saber: Fixed point controllers and stabilization of the cart-pole system and the rotating pendulum. In: Proc. 38th IEEE Conference on Decision and Control 1999, Vol. 2, pp. 1174–1181. DOI:10.1109/cdc.1999.830086

[23] R. Olfati-Saber: Normal forms for underactuated mechanical systems with symmetry. IEEE Trans. Automat. Control *47* (2002), 2, 305–308. DOI:10.1109/9.983365

[24] T. Ortega, R. Villafuerte, C. Vázquez, and L. Freidovich: Performance without tweaking differentiators via a pr controller: Furuta pendulum case study. In: 2016 IEEE International Conference on Robotics and Automation (ICRA), pp. 3777–3782. DOI:10.1109/icra.2016.7487566

[25] L. B. Prasad, B. Tyagi, and H. O. Gupta: Optimal control of nonlinear inverted pendulum system using pid controller and lqr: Performance analysis without and with disturbance input. Int. J. Automat. Computing *11* (2014), 6, 661–670. DOI:10.1007/s11633-014-0818-1

[26] P. Seman, B. Rohal-Ilkiv, M. Salaj, et al.: Swinging up the furuta pendulum and its stabilization via model predictive control. J. Electr. Engrg. *64* (2013), 3, 152–158. DOI:10.2478/jee-2013-0022

[27] A. S. Shiriaev, L. B. Freidovich, A. Robertsson, R. Johansson, and A. Sandberg: Virtual-holonomic-constraints-based design of stable oscillations of furuta pendulum: Theory and experiments. IEEE Trans. Robotics *23* (2007), 4, 827–832. DOI:10.1109/tro.2007.900597

[28] A. van der Schaft: Port-hamiltonian systems: an introductory survey. In: Proc. International Congress of Mathematicians (M. Sanz-Sole, J. Soria, J.L. Varona, and J. Verdera, eds.), Vol. III: Invited Lectures, Mathematical Society Publishing House, pp. 1339–1365, Madrid 2006. DOI:10.4171/022-3/65

[29] M. A. Vásquez-Beltrán and H. Rodríguez-Cortés: A total energy control system strategy for the quadrotor helicopter. In: International Conference on Unmanned Aircraft Systems 2015. DOI:10.1109/icuas.2015.7152302

H. Rodríguez-Cortés, Centro de Investigación y de Estudios Avanzados del Instituto Politécnico Nacional, Departamento de Ingeniería Eléctrica, Sección de Mecatrónica, Av. Instituto Politécnico Nacional 2508, Col. San Pedro Zacatenco, Ciudad de México. México.

e-mail: hrodriguez@cinvestav.mx